Journal of Alloys and Compounds 509 (2011) L142–L144

Contents lists available at ScienceDirect

Journal of Alloys and Compounds

journal homepage: www.elsevier.com/locate/jallcom

Letter

Hydrothermal synthesis of $Cu_3(OH)_2V_2O_7{\cdot}nH_2O$ nanoparticles and its application in lithium ion battery

Shibing Ni[a,*], Deyan He[b], Xuelin Yang[a], Tao Li[a]

[a] College of Mechanical and Material Engineering, Three Gorges University, 8 Daxue Road, Yichang 443002, PR China
[b] Department of Physics, Lanzhou University, Lanzhou 730000, PR China

ARTICLE INFO

Article history:
Received 7 July 2010
Received in revised form
16 December 2010
Accepted 19 December 2010
Available online 28 December 2010

Keywords:
Copper vanadium oxide hydroxide hydrate
Raman spectrum
Thermal analysis
Lithium ion battery

ABSTRACT

Well crystallized copper vanadium oxide hydroxide hydrate ($Cu_3(OH)_2V_2O_7{\cdot}nH_2O$) nanoparticles have been successfully synthesized by a simple hydrothermal method. The morphology and structure of the as-synthesized products were characterized by field emission scanning electron microscopy (FE-SEM), X-ray diffraction (XRD), Fourier transform infrared spectroscopy (FTIR), and Raman spectroscopy. The composition of $Cu_3(OH)_2V_2O_7{\cdot}nH_2O$ was studied by thermal analysis (TG, DTA), which indicates that there are two molecules of water in a $Cu_3(OH)_2V_2O_7{\cdot}nH_2O$ molecular formula. Electrochemical properties of $Cu_3(OH)_2V_2O_7{\cdot}2H_2O$ nanoparticles as positive electrode of lithium ion battery were studied by conventional charge/discharge tests at different current density, showing steady initial discharge platforms near 1.7 V. The first discharge capacity of $Cu_3(OH)_2V_2O_7{\cdot}2H_2O$ electrode arrives at 868 and 845 mAh g^{-1} at current density of 0.01 and 0.02 mA cm^{-2}, respectively.

1. Introduction

During the past few years, vanadium oxides based materials have attracted much attention due to their fascinating structures and electronic, optical, and magnetic properties, which are relevant to such diverse areas as lubrication, chemical sensor, catalysis, cathode materials in batteries, and minerals [1–6].

Stimulated by those applications, much work has been done on the synthesis and characterization of various vanadium compounds such as single crystallized $Ag_2V_4O_{11}$ [7], $K_2SrV_3O_9$ [8], $[\{M(H_2O)_2\}V_2O_6]$ (M = Co, Ni) [9], and $Zn_3(OH)_2V_2O_7{\cdot}nH_2O$ [10]. As a mineral known since the 18th century, $Cu_3(OH)_2V_2O_7{\cdot}nH_2O$ can now be prepared in laboratory via an aqueous solution method [11–13]. It has a novel structure that consist of alternated Cu–O layer and V–O layer with channels in V–O layer, which is similar with that of $Zn_3(OH)_2V_2O_7{\cdot}nH_2O$ [14–19]. Such a channel structure will facilitate the insertion and extraction, making $Cu_3(OH)_2V_2O_7{\cdot}nH_2O$ to have potential applications as positive electrode in lithium ion battery. However, up to now, limited reports about $Cu_3(OH)_2V_2O_7{\cdot}nH_2O$ was mainly focused on the synthesis method research and structure characterization, few attention has been paid to the electrochemical performance of $Cu_3(OH)_2V_2O_7{\cdot}nH_2O$ by now.

We have reported hydrothermal synthesis of $Cu_3(OH)_2V_2O_7{\cdot}nH_2O$ and its magnetism [20]. In this paper, we will investigate the application of $Cu_3(OH)_2V_2O_7{\cdot}nH_2O$ nanoparticles as positive electrode for lithium ion battery.

2. Experimental

All the chemicals were of analytical grade and purchased from Shanghai Chemical Reagents. In a typical process, 1 mmol V_2O_5, 5 mmol hexamethylenetetramine and 3 mmol $Cu(NO_3)_2$ were dissolved in 30 ml distilled water, then 0.5 g sodium sulfate was put into the solution. After stirring for 20 min, the obtained homogeneous yellowy suspension was transferred into a 50 ml teflonlined autoclave, distilled water was subsequently added up to 80% of its capacity. The autoclave was at last sealed and placed in an oven, heated at 140 °C for 24 h. The autoclave was cooled in air. The precipitate was centrifuged with distilled water and ethanol for 4 times and dried in an oven at 60 °C for 24 h [20].

The morphology, structure and composition of the products were characterized by field-emission scanning electron microscopy (FE-SEM S-4800, Hitachi) equipped with energy dispersion spectrum (EDS), X-ray powder diffraction (Rigaku RINT2400 with Cu Kα radiation), Fourier transform infrared spectroscopy (IFS 66 V/S Bruker, Germany), and micro-Raman spectrometer (Jobin Yvon LabRAM HR800 UV, YGA 532 nm). For fabricating of Li-ion battery, a mixture of $Cu_3(OH)_2V_2O_7{\cdot}nH_2O$ (80 wt%), acetylene black (10 wt%), and polyvinylidene fluoride (PVDF, 10 wt%) electrodes were drying (120 °C, 24 h, vacuum) and compressed on copper foil. Coin-type cells (2032) of Li/1 M $LiPF_6$ in ethylene carbonate, dimethyl carbonate and ethylmethyl carbonate (EC/DMC/EMC, 1:1:1, v/v/v)/$Cu_3(OH)_2V_2O_7{\cdot}nH_2O$ were assembled in an argon-filled dry box. A Celgard 2320 microporous polypropylene was used as the separator membrane. The cells were tested in the voltage range between 0.02 and 3 V with a multichannel battery test system (NewareBTS-610).

* Corresponding author. Fax: +86 717 6396559.
E-mail address: shibingni07@gmail.com (S. Ni).

0925-8388/$ – see front matter © 2010 Elsevier B.V. All rights reserved.
doi:10.1016/j.jallcom.2010.12.139

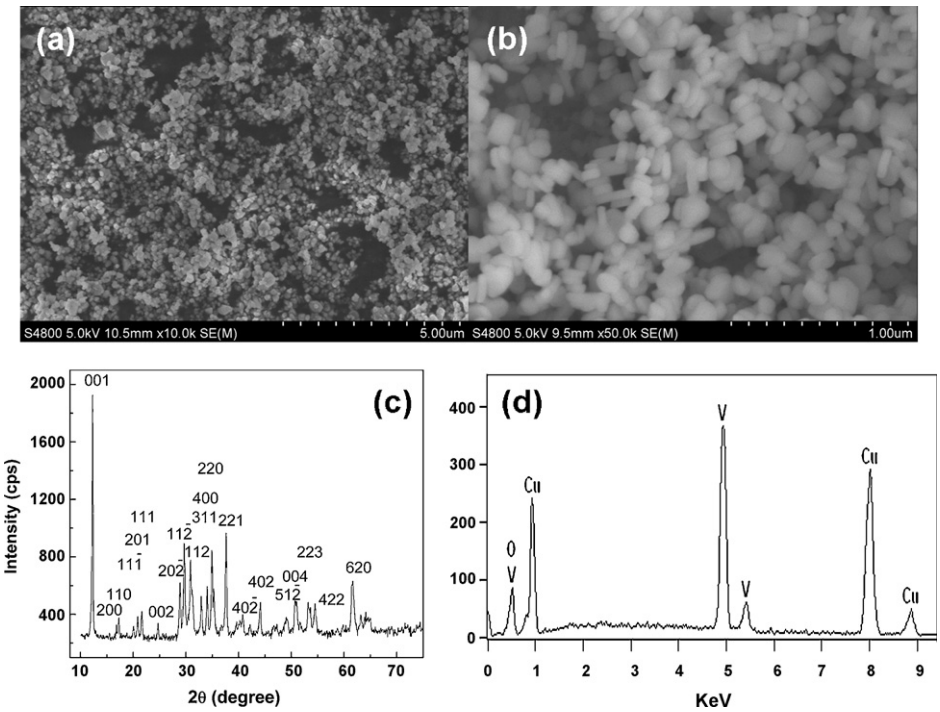

Fig. 1. SEM images of the products in low (a) and higher (b) magnification; (c) XRD pattern and (d) EDS spectrum of the sample.

3. Results and discussion

SEM images of the products are shown in Fig. 1. Fig. 1(a) is a low magnification of the products, which exhibits a large quantity of nanoparticles. The mean diameter of those nanoparticles is about 100 nm. Higher magnification SEM image is shown in Fig. 1(b), which exhibits smooth surfaces and symmetrical size distribution. The typical X-ray diffraction pattern of the as-synthesized products is shown in Fig. 1(c). All diffraction peaks can be indexed as the monoclinic phase of $Cu_3(OH)_2V_2O_7{\cdot}nH_2O$ with the lattice constants $a = 1.061$ nm, $b = 0.586$ nm, and $c = 0.7260$ nm, which is in good agreement with the JCPDS, no. 46-1443. Strong and sharp peaks suggest that the as-synthesized products are well crystallized. EDS was employed for further investigation of the compositions of the products, which is shown in Fig. 1(d). V, Cu and O elements are clearly observed from the EDS spectrum, which is in accordance with the composition of $Cu_3(OH)_2V_2O_7{\cdot}nH_2O$. The reactions during the hydrothermal process are likely to be as follows:

$$(CH_2)_6N_4 + 10H_2O \rightarrow 6HCHO + 4NH_3{\cdot}H_2O \quad (1)$$

$$NH_3{\cdot}H_2O \rightarrow OH^- + [NH_4]^+ \quad (2)$$

$$V_2O_5 + (2n+2)OH^- + 3Cu^{2+} + (2n-4)H^+ \rightarrow Cu_3(OH)_2V_2O_7{\cdot}nH_2O + (n-2)H_2O \quad (3)$$

Fig. 2 shows the infrared spectrum and Raman spectrum of the as-prepared copper pyrovanadate. As shown in infrared spectrum in the wavelength region of 300–4000 cm^{-1}, the high wavenumber vibration located at 3531, 3470 and 3044 cm^{-1} correspond to water and hydroxyls vibration modes, and the low wavenumber vibration located at 900, 847, 804, 763, 562, 531, 505 and 419 cm^{-1} are attributed to tetrahedral VO_4 and octahedral CuO_6 vibration modes in the network. The vibration located at 1012, 1409, 1437, 1920 and 1974 cm^{-1} may ascribe to HCO_3^- that derives from hexamethylenetetramine [21]. It shows similar vibration with that reported in the literature for copper pyrovanadate [18]. Raman spectrum in the wavelength range of 150–1150 cm^{-1} is dominated by Raman peaks located at 164, 236, 342, 438, 476, 758, 820, and 894 cm^{-1}, and these peaks are the vibration bands of $Cu_3(OH)_2V_2O_7{\cdot}nH_2O$. We suggest the peaks at 476, 758, 820, and 894 cm^{-1} are attributed to V–O vibration, the peaks at 164 and 236 cm^{-1} are caused by the symmetry-related vibration [22–24], and the peak at 438 cm^{-1} comes from Cu–O vibration [25]. IR vibrations of $Cu_3(OH)_2V_2O_7{\cdot}nH_2O$ are inevitably of little shift in wavenumber region due to the wide range. Infrared spectrum and Raman spectrum of the product are well in agreement with its crystal structure.

The thermal behavior of $Cu_3(OH)_2V_2O_7{\cdot}nH_2O$ is investigated by means of TG/DTA measurement in Ar atmosphere at a heating rate of 10 K min^{-1} (Fig. 3). The TG curve shows weight losses between 300 and 970 K, which are relevant to the elimination of water molecules and the phase transformation. The dehydration and decomposition steps are observed in two areas: 350–520 K and 520–600 K. The corresponding observed weight losses are 7.81% and 3.9% by mass and total weight loss is 11.71%. The first step

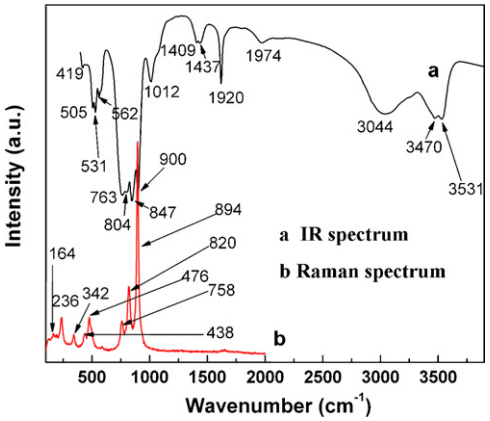

Fig. 2. FTIR spectrum and Raman spectrum of the products.

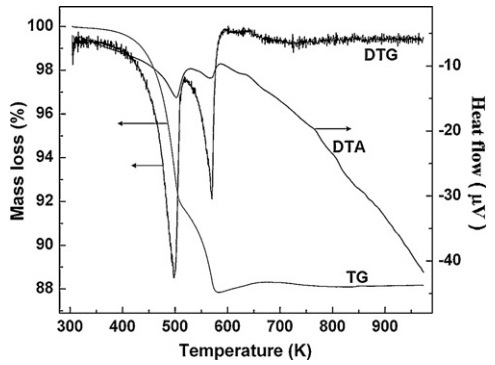

Fig. 3. TG, DTA, DTG curves of the products at N_2 atmosphere.

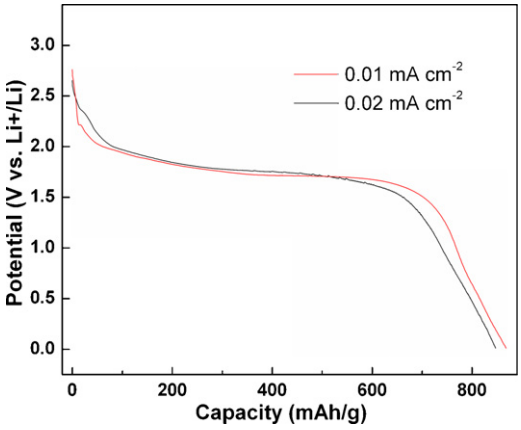

Fig. 4. First discharge curves of the electrode made of $Cu_3(OH)_2V_2O_7{\cdot}nH_2O$ nanoparticles at different current density.

of weight loss corresponds to the elimination of water and the second one corresponds to the elimination of hydroxyl, which indicates there are two moleculars of water in a $Cu_3(OH)_2V_2O_7{\cdot}nH_2O$ molecular formula. The thermal behavior can be testified from two continuous endothermic peaks on DTG curves that are observed at 496 K and 569 K. The DTA curve shows two peaks at 506 K and 568 K, which are relevant to the elimination of water and the decomposition of copper vanadium oxide. The reactions during the thermal process are likely to be as follows:

$$Cu_3(OH)_2V_2O_7{\cdot}2H_2O \rightarrow Cu_3(OH)_2V_2O_7 + 2H_2O \rightarrow Cu_3(VO_4)_2 + H_2O \quad (4)$$

Fig. 4 shows the first discharge curves of a $Cu_3(OH)_2V_2O_7{\cdot}2H_2O$ electrode at current density of 0.01 and 0.02 mA cm^{-2}. It shows a high initial discharge capacity of 868 and 845 mAh g^{-1} at current density of 0.01 and 0.02 mA cm^{-2}, which is bigger than that reported in literature [26]. The initial discharge curves of $Cu_3(OH)_2V_2O_7{\cdot}2H_2O$ electrode show steady platforms near 1.7 V ranging from 100 to 600 mAh g^{-1}, being similar with that reported in literature [26]. This result suggests $Cu_3(OH)_2V_2O_7{\cdot}2H_2O$ as an ideal candidate of positive material for lithium ion batteries.

4. Conclusion

In conclusion, novel channel structured $Cu_3(OH)_2V_2O_7{\cdot}2H_2O$ nanoparticles were synthesized by a simple hydrothermal method. Discharge curve shows steady platform, suggesting it as an ideal candidate of positive material for lithium ion batteries. As it is well known that the morphology and size have important effects on the physical and chemical properties of nanomaterial, promising work should be done on the morphology and size controlled fabrication to optimize the electrochemical performance of $Cu_3(OH)_2V_2O_7{\cdot}2H_2O$.

Acknowledgements

We gratefully acknowledge the financial support from the Teaching and Research Award Program for Outstanding Young Teachers (MOE, China), Natural Science Foundation of China (NSFC, 50972075), Key projects of Chinese Ministry of Education (D209083), and Education Office of Hubei Province (D20081304 and CXY2009A004). Moreover, the authors are grateful to Dr. Jianlin Li at Three Gorges University for his kind support to our research.

References

[1] E. Lugscheider, O. Knotek, K. Bobzin, S. Barwulf, Surf. Coat. Technol. 133/134 (2001) 362.
[2] A. Lavacchi, B. Cortigiani, G. Rovida, U. Bardi, A. Atrei, R. Angelucci, Sens. Actuators B 71 (2000) 123.
[3] W.P. Griffith, Trans. Met. Chem. 16 (1991) 548.
[4] I.V. Kozhevnikov, Chem. Rev. 56 (1987) 811.
[5] M. Zhang, J.R. Dahn, J. Electrochem. Soc. 143 (1996) 2730.
[6] H.T. Evans, J.A. Konnert, Am. Mineral. 63 (1978) 863.
[7] C.J. Mao, X.C. Wu, H.C. Pan, J.J. Zhu, H.Y. Chen, Nanotechnology 16 (2005) 2892.
[8] A.A. Tsirlin, V.V. Chernaya, R.V. Shpanchenko, E.V. Antipov, J. Hadermann, Mater. Res. Bull. 40 (2005) 800.
[9] M.I. Khana, S. Deba, V.O. Golubb, C.J. O'Connorb, R.J. Doedens, J. Mol. Struct. 707 (2004) 217.
[10] S.B. Ni, S.M. Lin, Q.T. Pan, K. Huang, F. Yang, D.Y. He, J. Alloys Compd. 477 (2009) L1.
[11] N. Strupler, Ann. Chim. 10 (1965) 345.
[12] K. Melghit, B. Belloui, A.H. Yahya, J. Mater. Chem. 9 (1999) 1543.
[13] K. Melghit, A.H. Yahaya, I.I. Yaacob, Mater. Lett. 57 (2003) 1423.
[14] P.Y. Zavalij, F. Zhang, M.S. Whittingham, Acta Crystallogr. C53 (1997) 1738.
[15] P.Y. Zavalij, F. Zhang, M.S. Whittingham, Solid State Sci. 4 (2002) 591.
[16] D. Hoyos, L.A. Palacio, J.L. Paillaud, A.S. Simon-Masseron, J.L. Guth, Solid State Sci. 6 (2004) 1251.
[17] K. Melghit, A.K. Al-Belushi, I. Al-Amri, Ceram. Int. 33 (2007) 285.
[18] K. Melghit, C. R. Chimie 11 (2008) 317.
[19] S.B. Ni, G. Zhou, S.M. Lin, X.H. Wang, Q.T. Pan, F. Yang, D.Y. He, Mater. Lett. 63 (2009) 2459.
[20] S.B. Ni, X.H. Wang, G. Zhou, F. Yang, J.M. Wang, D.Y. He, Mater. Lett. 64 (2010) 516.
[21] M. Zhang, E.R. Maddrell, P.K. Abraitis, E.K.H. Salje, Mater. Sci. Eng. B 137 (2007) 149.
[22] P.K.L. Au, C. Calvo, Can. J. Chem. 45 (1967) 2297.
[23] R. Gopal, C. Calvo, Can. J. Chem. 51 (1973) 1004.
[24] R. Gopal, C. Calvo, Acta Crystallogr. 830 (1974) 2491.
[25] R. Wahab, S.G. Ansari, Y.S. Kima, H.K. Seo, G.S. Kima, G. Khang, H.S. Shin, Mater. Res. Bull. 42 (2007) 1640.
[26] X.J. Sun, J.W. Wang, Y. Xing, Y. Zhao, X.C. Liu, B. Liu, S.Y. Hou, Cryst. Eng. Commun. 13 (2011) 367.